Calculation of intersubband absorption in doped graded quantum wells under intense terahertz irradiation

A. Hernández-Cabrera[*] and P. Aceituno

Dpto. Física Básica, Universidad de La Laguna, La Laguna, 38206-Tenerife, Spain

In this work, the intersubband absorption is studied in a δ-doped graded quantum well structure with very close excited levels when this structure is subjected to a very intense terahertz irradiation. Multiple peak structure of the absorption is essentially modified by the strong oscillation of deepest excited levels, which periodically changes their energy proximity, and by the appearance of the so-called "forbidden" transitions. Effects generated by the oscillatory population of the deepest subbands have been considered. Calculations have been done within the matrix density formalism and the adiabatic approach, taking into account self-consistently electronic levels and depolarization contribution to levels shift. Relaxation rates dependence on terahertz irradiation and charge concentration has been considered.

I. INTRODUCTION

It is known that very intense transverse fields considerably modify confined states of quantum nanostructures.[1] A conventional method to study these modifications is the interband optical absorption.[2–4] To analyze in a quantitative way the interband response, it is necessary not only to consider modifications of the electron and hole states, but also excitonic effects. However, when the electronic excitation is in the infrared (IR) range, the intersubband response between electronic states of the conduction band becomes relevant.[4] A quite interesting case, but little studied, is that the modification of the intersubband transitions caused by a very intense terahertz irradiation.[5] The aforementioned irradiation can be achieved experimentally by using gas or free-electron lasers (FEL) with energy densities of megawatt cm^{-2}. These lasers have already been used to study the response of different types of nanostructures.[6,7] Heterostructures with closely spaced levels, such as stepped quantum wells (SQWs) or graded quantum wells (GQWs) have been investigated through optical and transport methods during the past decade.[8] Recently, photoluminescence and photocurrent measurements have been reported for GQWs.[9] The interlevel population inversion in such structures due to the heating caused by a longitudinal electric field is analyzed in Refs. [10] and [11]. One of the most attractive features of GQWs that distinguished them from other quantum structures is the narrow bandwidth of their intersubband optical transition. Thus, GQWs are appropriate for the application as tunable optical semiconductor devices including far-infrared lasers. The task of the current work is to show peculiarities in graded quantum wells when doped, because these structures show an intricate response under specific stimuli, as intense terahertz irradiation.

Let us suppose we subject a GQW to an intense terahertz irradiation. The GQW is formed by a GaAs narrow well, of width d, in the center of a $Ga_{0.65}Al_{0.35}As$ wide well, of width D. Finite AlAs barriers flank the wide well [see Fig. 1(a)]. If the structure undergoes a transverse terahertz electric field $E_\perp(t) = E_\omega \cos \omega t$ [Fig. 1(b)], the electronic response can be studied within the adiabatic approximation whenever $\hbar \omega$

$\ll \varepsilon_{ji}$, ε_{ji} being the interlevel energy distance between the jth and ith levels. However, in the present scenario, since $|e|E_\omega D/2\varepsilon_{ji}$, we cannot consider the radiation as a perturbation and we will have to describe electronic states numerically. For structures with closely spaced levels, when $\varepsilon_{ji} < \hbar \omega$, the intersubband transitions are excited in far-infrared spectral region. The shape of the absorption peak is mainly controlled by effect of the Coulomb interaction or by the elastic scattering of electrons in heterostructure defects. Coulomb interaction on intersubband transitions in two-dimensional (2D) systems has different symptoms. One of them is the depolarization shift of the spectrum caused by the dynamic screening of the infrared field by electrons.[12] However, exchange interaction opposes to the former interaction
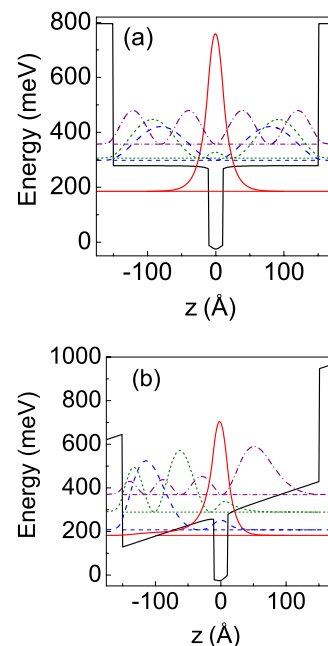

FIG. 1. (Color online) Graded quantum well under terahertz irradiation with the four deepest energy levels. Corresponding wave functions are included. (a) $E_\omega = 0$ kV/cm. (b) $E_\omega = 100$ kV/cm and $\omega t = \pi$.

reducing depolarization shift and absorption shape appears unchanged.

Due to the external field, electronic levels will oscillate with a frequency ω, causing the $(n+1)$-order intersubband transitions and the consequent fine structure of the absorption. Here, n is the number of terahertz photons, while we only have a single infrared photon corresponding to the probe field. Moreover, a considerable modification of the shape of the absorption peaks appears due to relaxation of the levels and depolarization.

II. INTERSUBBAND RESPONSE

Present calculations are based on the one-particle density matrix, linearized with respect to the probe IR field $E_\Omega \exp(-i\Omega t)$. The method was already developed elsewhere and we will not extend ourselves in detailing the theoretical process to calculate the absorption.[5] We will describe levels broadening in a phenomenological way considering longitudinal optical (LO) phonon emission in the spectral region $\Omega > \omega_{LO}$, ω_{LO} being the longitudinal optical phonon frequency. Also, we will take into account depolarization contribution to broadening. If we consider a system with $j+1$ levels excited by a far-infrared radiation (the deep populated and j excited conduction levels), perpendicularly directed to the 2D plane, the induced transverse current can be calculated through the density matrix $\hat{\rho}(t)$ as $j_\perp(t) = \sum_j e\rho_{2D} v_{1j}(t) \int_0^\infty d\varepsilon\, \delta f_{1j}(\varepsilon,t)$, where $\delta f_{1j}(\varepsilon,t) = \langle \varphi^1(z,t) | \hat{\rho}(\varepsilon,t) | \varphi^j(z,t) \rangle$ are the nondiagonal terms of the density matrix, $v_{1j}(t) = -i\omega_{j1} \langle \varphi^1(z,t) | z | \varphi^j(z,t) \rangle$ are the intersubband matrix elements of the transverse velocity operator, $\varphi^k(z,t)$ are the electronic wave functions in the k subband, ρ_{2D} is the 2D density of states, and $\varepsilon = p^2/2m$ is the kinetic energy for the in-plane motion. If we assume that the problem has in-plane isotropy, the density matrix only depends on ε. The relative absorption $\xi(t)$ can be defined as the ratio of the absorbed power $\text{Re}[E_\perp(t) j_\perp(t)]$ to the Poynting vector for the radiation across the structure, and can be written as $\xi(t) = \frac{e^2}{c\sqrt{\epsilon}} \sum_j \frac{4m|v_{1j}(t)|^2}{\omega_{j1}} \text{Im} \int_0^\infty d\varepsilon\, \Phi(\varepsilon)$, where ϵ is the dielectric permittivity, and $\Phi(\varepsilon)$ is the normalized intersubband polarization which can be deduced from the matrix density as $\delta f_{1j}(\varepsilon,t) = -(\frac{ie}{\omega_{j1}}) E_\perp(t) v_{12}(t) \Phi(\varepsilon)$.

To calculate the electronic states, we need to solve the eigenvalue Schrödinger equation. It is convenient to use the parametrically time-dependent wave functions, $\varphi^k(z,t)$, determined by the eigenstate problem:

$$\hat{H}(z,t)\varphi^k(z,t) = \varepsilon_k(t)\varphi^k(z,t), \tag{1}$$

and

$$\hat{H}(z,t) = \frac{\hat{p}_z^2}{2m} + V_{GQW}(z) + V_H(z,t) + V_{xc}(z,t) + ezE_\omega \cos \omega t. \tag{2}$$

Here, m is the electron effective mass in the growth direction, and $V_{GQW}(z)$, $V_H(z,t)$, and $V_{xc}(z,t)$ are the GQW, Hartree, and Fock potential terms, respectively. Equation (1) must be solved together with the Poisson equation for each

value of t. The standard self-consistent numerical procedure for this eigenstate problem involves the Hartree potential $V_H(z,t)$, which is obtained from the Poisson equation,

$$\frac{d^2 V_H(z,t)}{dz^2} = \frac{4\pi e^2}{\epsilon} \left[N_D(z) - \sum_j n_j(t) |\varphi^j(z,t)|^2 \right]. \tag{3}$$

Here, $N_D(z)$ is the doping profile of donors, coming from the δ doping, ϵ is the dielectric permittivity that we have supposed as uniform across the heterostructure, and

$$n_j(t) = \frac{mk_BT}{\pi\hbar^2} \ln\left[1 + \exp\left(\frac{\varepsilon_F - \varepsilon_j(t)}{k_BT} \right) \right]. \tag{4}$$

Therefore, $\int N_D(z) dz = \sum_j n_j(t) = n_{2D}$ is the in-plane averaged 2D density of electrons (donors) and j refers to the occupied subbands. The Fermi energy, ε_F, is expressed through the total electron density n_{2D}.

The Fock term,

$$V_{xc}(z,t) = \frac{e^2}{\epsilon} \int dz' \frac{1}{|z-z'|} \varphi^{*j}(z',t)\varphi^j(z,t), \tag{5}$$

includes exchange contribution.[13] This contribution strongly affects wave functions for high densities, as in our case. For high doping concentration, the attractive space-charge potential energy created by the spatial distribution is noticeable. The Hartree-Fock approximation used here for the many-body Coulomb potential energy incorporates the main peculiarities of the particle interactions as function of the carrier densities. Thus, when the carrier density increases, the repulsive part of the Hartree-Fock potential energy increases as well. Beyond a certain electronic density, the repulsion compensates the attractive Coulomb interaction and the intersubband shift due to the Coulomb renormalization.[13–15]

Finally, $ezE_\omega \cos \omega t$ is the terahertz energy contribution. We will consider the IR field by means of the perturbation operator $\delta\hat{H}(z,t) = \frac{ie}{\Omega} E(\Omega)\hat{v}(z,t)$.

To solve Eqs. (1)–(5), we have used the continuity conditions for wave functions and current at each interface

$$\varphi_\alpha^k(z,t)\big|_{z=L_i} = \varphi_\beta^k(z,t)\big|_{z=L_i},$$

$$\frac{1}{m_\alpha} \frac{\partial \varphi_\alpha^k(z,t)}{\partial z}\bigg|_{z=L_i} = \frac{1}{m_\beta} \frac{\partial \varphi_\beta^k(z,t)}{\partial z}\bigg|_{z=L_i}, \tag{6}$$

where subindices α, β refer to materials forming each interface at L_i position. Although underbarrier penetration slightly modifies wave functions and energy levels position, we have taken into account this possibility using barriers of finite height in calculations.

Some authors assure the depolarization shift on the absorption is noticeable for high doped QWs.[16,17] We have included numerical calculations of these effects (see Appendix A) based on a time-adapted version of expression (17) in Ref. 16,
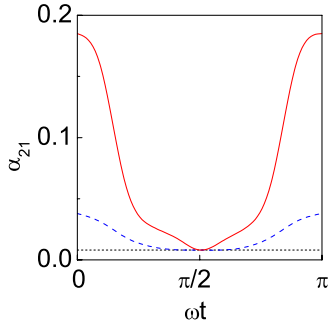
FIG. 2. (Color online) Time dependence of dimensionless depolarization for $E_\omega=100$ kV/cm (solid line), $E_\omega=80$ kV/cm (dashed line), and $E_\omega=20$ kV/cm (dotted line).

$$\alpha_{j1}(t) = \frac{8\pi e^2(n_1(t) - n_j(t))}{\epsilon[\varepsilon_{j1}(t)]} \int_{-\infty}^{\infty} dz \left[\int_{-\infty}^{z} dz' \varphi^j(z',t)\varphi^1(z,t) \right]^2,$$

(7)

where $\varepsilon_{j1}(t) = \varepsilon_j(t) - \varepsilon_1(t)$. Similar expression can be found in Batista *et al.*[18] for the case of time-independent wave functions. We have represented in Fig. 2 the evolution of the dimensionless depolarization $\alpha_{j1}(t)$ for different terahertz fields. Following the above references interlevel energy modifications caused by the depolarization can be expressed through $\widetilde{\varepsilon}_{j1}(t) = \varepsilon_{j1}(t)[1 + \alpha_{j1}(t)]^{1/2}$. Because the energy corrections due to the dimensionless depolarization shift can be of the order of 9.5%, we cannot ignore this contribution for $1 \rightarrow 2$ transition. Although expression (17) of Załużny only considers a two-band model, we have extended it to estimate the contribution for $1 \rightarrow 3$ transition, and depolarization shift is negligible for this case (0.05%). We have used in calculations a thermal energy $k_B T = 0.4$ meV, corresponding to $T = 4.8$ K.

With the above considerations, we have calculated wave functions and subband energy values. We have used in calculations a set of ten decoupled GQW. Each GQW is composed by a 25 Å narrow well, placed in the center of a 300 Å wide well, and doped with a δ-donor doping in its center, in such a way that only the ground state (corresponding to the first level in the conduction band) is populated. In our case, the electronic density is $n_{2D} = 5.5 \times 10^{12}$ cm^{-2}. Well sizes have been deliberately chosen so that the two deepest excited states (second and third conduction states) are very close in energy for zero terahertz field. Since the electric field of the radiation breaks the symmetry of wave functions, zero-field "forbidden" transition between the first and third levels becomes allowed. This transition, together with the intense irradiation, will provide us the fine structure of a quite complex relative absorption. We have considered a terahertz electric field with amplitude E_ω varying between 0 and 100 kV/cm. Figure 1 shows the shape of the GQW subjected to the limiting cases of terahertz fields: $E_\omega = 0$ kV/cm (*a*) and $E_\omega = 100$ kV/cm for $\omega t = \pi$ (*b*). The first four levels and the corresponding wave functions are also shown for both cases. For 0 kV/cm field, one can observe that the energy gap between the first-excited and the ground levels, $\widetilde{\varepsilon}_{21}(t)$ is 113 meV, while the energy gap between the
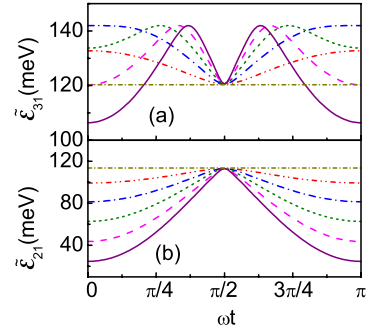

FIG. 3. (Color online) Time dependence of interlevel energy distance for the $1 \rightarrow 2$ and $1 \rightarrow 3$ transitions. $E_\omega=0$ kV/cm (short dash-dot), $E_\omega=20$ kV/cm (dash-dot-dot), $E_\omega=40$ kV/cm (dash-dot), $E_\omega=60$ kV/cm (dot), $E_\omega=80$ kV/cm (dash), and $E_\omega=100$ kV/cm (solid).

two excited levels $\widetilde{\varepsilon}_{32}(t)$ is about 8 meV. However, when increasing the electric field, the first-excited level moves a bigger energy amount than the others, becoming close to the ground state: $\widetilde{\varepsilon}_{21}(t = \pi/\omega)$ diminishes to 25 meV, while $\widetilde{\varepsilon}_{32}(t = \pi/\omega) = 82$ meV for $E_\omega=100$ kV/cm. Since the field depends on ωt, the distance between levels will oscillate between these extreme values. We will not take into consideration the third excited level $\widetilde{\varepsilon}_4(t)$ because it is separated enough from $\widetilde{\varepsilon}_3(t)$.

Figure 3 shows $\widetilde{\varepsilon}_{j1}(t)$ variation versus ωt. One can see that the temporal complexity of wave functions and levels does not allow us to use the parabolic approximation, in which wave functions and levels can be developed in cosine series as[5]

$$\varphi^k(z,t) = \varphi^k(z) + \sum_{k' \neq k} \frac{eE_\omega z_{kk'}}{\varepsilon_k - \varepsilon_{k'}} \varphi^{k'}(z)\cos\omega t + \cdots,$$

$$\varepsilon_k(t) \simeq \varepsilon_k + eE_\omega z_{kk}\cos\omega t + \sum_{k' \neq k} \frac{|eE_\omega z_{kk'}|^2}{\varepsilon_k - \varepsilon_{k'}}\cos^2\omega t. \quad (8)$$

III. RELATIVE ABSORPTION

To calculate the relative IR absorption, averaged over the terahertz pump, we first deduce the high-frequency contribution, $\Delta\rho_\mathbf{p}(z,z',t)\exp(-i\Omega t)$, from the matrix density in the coordinate-momentum representation. This contribution is described by the linearized equation

$$\frac{\partial \Delta\rho_\mathbf{p}(z,z',t)}{\partial t} + \frac{i}{\hbar}[\hat{H}(z,t) - \hat{H}(z',t) - \hbar\Omega]\Delta\rho_\mathbf{p}(z,z',t)$$

$$+ \frac{i}{\hbar}[\widehat{\delta H}(z) - \widehat{\delta H}(z')]\rho_\mathbf{p}(z,z',t) = 0, \quad (9)$$

where z is the transverse coordinate (growth direction) and $\mathbf{p}$ is the two-dimensional momentum. Following Ref. 5, we can obtain the time-dependent photoinduced current through the density matrix as

$$j(t) = \frac{e}{L^2} \sum_{\mathbf{p}} \int_{-d/2}^{d/2} dz \lim_{\varsigma,\varsigma' \to z} [\hat{v}(\varsigma) + \hat{v}(\varsigma')] \Delta \rho_{\mathbf{p}}(\varsigma, \varsigma', t)$$

$$= \frac{2e}{L^2} \sum_{\mathbf{p}kk'} v_{k'k}(t) \Delta \rho_{\mathbf{p}}(k, k', t), \tag{10}$$

where L^2 is the normalization area and $v_{kk'}(t)$ $= \int_{-d/2}^{d/2} dz \varphi^{k*}(z, t) \hat{v}(z) \varphi^{k'}(z, t)$ is the interlevel electronic velocity. For the case of resonant excitation between the ground and the jth levels, when $\hbar\Omega \simeq \tilde{\varepsilon}_{j1}$, Eq. (7) becomes $j(t)$ $\simeq ev_{1j}(t) \Delta \rho(j, 1, t)$. To obtain this result, we have made the sum over 2D momentum according to $\Delta\rho(j, 1, t)$ $= (2/L^2) \Sigma_{\mathbf{p}} \Delta \rho_{\mathbf{p}}(j, 1, t)$. If only the ground level is populated, we can write from Eq. (7) the differential equation for $\Delta\rho(j, 1, t)$ as

$$\frac{\partial \Delta\rho(j, 1, t)}{\partial t} + i[\Omega_{j1}(t) - \Omega - i\nu_{j1}(t)] \Delta\rho(j, 1, t) = \frac{eE_\Omega}{\hbar\Omega} v_{j1}(t) n_{2\mathrm{D}}, \tag{11}$$

where $\Omega_{j1}(t) = [\tilde{\varepsilon}_j(t) - \tilde{\varepsilon}_1(t)]/\hbar$ is the time-dependent interlevel frequency, and $\nu_{j1}(t) = \nu_\Omega(t)$ is the effective (see Appendix A) relaxation frequency. Solving Eqs. (9)–(11) and using the generalized Ohm tensorial law

$$j_i(t) = \sigma_i^j(t) E_j(t), \tag{12}$$

which, in the present case, is simplified to $\sigma_\Omega(t) = j(t)/E_\Omega$, we obtain the conductivity

$$\sigma_\Omega(t) = \frac{e^2 n_{2\mathrm{D}}}{\hbar\Omega} \sum_{j=2,3} v_{j1}(t) \int_{-\infty}^{t} dt' v_{j1}(t')$$

$$\times \exp\{-i \int_{t'}^{t} d\tau [\Omega_{j1}(\tau) - \Omega - i\nu_\Omega(\tau)]\}. \tag{13}$$

Finally, if we average throughout a period we obtain the relative absorption

$$\xi_\Omega = \frac{4\pi}{c\sqrt{\epsilon}} \mathrm{Re} \int_{-\pi/\omega}^{\pi/\omega} \frac{dt}{2\pi/\omega} \sigma_\Omega(t). \tag{14}$$

Therefore, we calculate the electronic velocity between the involved levels, and the relaxation frequency. In the present context, it is possible to use the adiabatic approach since the condition $\hbar\omega \ll \tilde{\varepsilon}_{ji}$ is fulfilled for ω of terahertz because we have considered a quanta terahertz energy $\hbar\omega = 1.5$ meV. However, integrals appearing in the conductivity and relative absorption must be solved numerically. Also, we have found that velocity matrix elements, $v_{j1}(t)$, strongly depend on t. In wide enough wells, this situation takes place even for low fields. Since we are working with 300 Å GaAs wells, this will be the general bearing. The calculations of the relative absorption have been carried out considering a structure of ten decoupled GQW to increase the absolute value of the absorption.

We have also taken into account a stepped relaxation energy, considering a value in the passive region (elastic scattering with acoustic phonons when $\hbar\Omega < \hbar\Omega_{\mathrm{LO}}$) which abruptly increases in the active ($\hbar\Omega > \hbar\Omega_{\mathrm{LO}}$) region due to the emission of longitudinal optic phonons. We include in
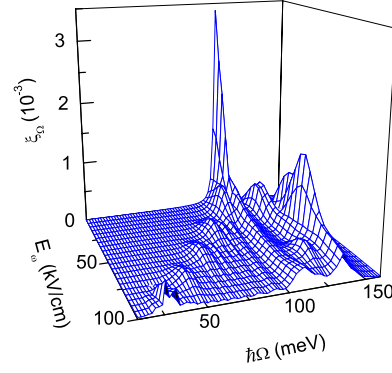

FIG. 4. (Color online) Relative absorption vs terahertz field and IR test energy.

Appendix B the study of electron-LO phonon interaction and elastic scattering under terahertz pump. For fixed ω and $n_{2\mathrm{D}}$ values, with $\hbar\Omega_{\mathrm{LO}} = 35$ meV, $\hbar\nu$ for the passive region remains practically constant within the terahertz field range used in this work, but it varies with the involved transitions. Thus, for transition $1 \to 2$, $\hbar\nu_{12} \simeq 0.66$ meV and for transition $1 \to 3$, $\hbar\nu_{13} \simeq 0.9$ meV. For the active region relaxation energy increases with terahertz field intensity from $\hbar\nu_{12} \simeq 1.4$ meV ($\hbar\nu_{13} \simeq 1.5$ meV) for low fields, to $\hbar\nu_{12} \simeq 1.8$ meV ($\hbar\nu_{13} \simeq 3.4$ meV) for $E_\omega = 100$ kV/cm.

We represent the evolution of the relative absorption in Figs. 4 and 5. The peak appearing at $E_\omega = 0$ kV/cm only corresponds to the $1 \to 2$ transition because $1 \to 3$ transition is forbidden for zero field due to the symmetry of the wave functions, as mentioned before. As soon as $E_\omega \neq 0$ kV/cm, the last transition appears and the absorption unfolds in two multiple peaks structure. We see that, in the vicinity of $\hbar\Omega = 117$ and 120 meV [values of $\tilde{\varepsilon}_{21}$ and $\tilde{\varepsilon}_{31}$, respectively, for $\cos(\omega t) = 0$] two very close peaks appear corresponding to both transitions. It is the region of the bigger approach of the levels. Starting from $E_\omega \simeq 30$ kV/cm, the relative absorption corresponding to the transition $1 \to 3$ becomes more marked although the structure of $1 \to 2$ is richer. Indeed, this bearing is caused by the increase of the interlevel velocity due to the wave functions overlap. It is important to point out that, although the first-excited level could be partially filled after excitation, contribution of the $2 \to 3$ transition is negligible in
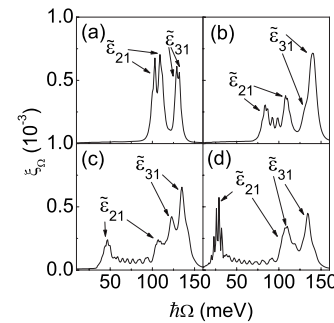

FIG. 5. Sections of the relative absorption for different terahertz fields. $E_w = 20$ kV/cm (a), $E_w = 40$ kV/cm (b), $E_w = 80$ kV/cm (c), and $E_w = 100$ kV/cm. (d) Arrows indicate the main contributions of each transition.
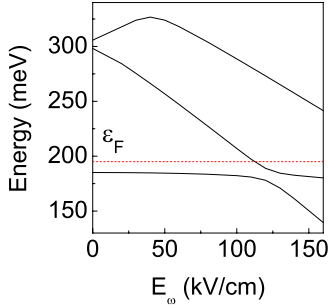
FIG. 6. (Color online) Energy levels vs E_ω for $\omega t=0$ showing the anticrossing. Dotted line represents the Fermi level.

our calculations. This is due to a worthless interlevel redistribution under terahertz pump because the interlevel energy $\widetilde{\varepsilon}_{21}$ is bigger than 25 meV while the terahertz quanta energy $\hbar\omega$ is around 1.5 meV.

What happens beyond $E_\omega=100$ kV/cm? If energy levels are represented as function of the terahertz electric field for $\omega t=0$ (Fig. 6), a typical anticrossing of the two deepest levels appears at $E_\omega \simeq 120$ kV/cm. Both levels decrease as the field increases falling down under the Fermi level beyond the anticrossing. This means that both subbands are occupied and transition $1\rightarrow2$ cannot be expected to happen. At the same time, transition $2\rightarrow3$ enhances its contribution becoming noticeable.

In order to show the relative absorption behavior for this situation, we have performed calculations for $E_\omega=140$ kV/cm with the general terahertz temporal evolution $E_\perp(t)=E_\omega \cos\omega t$. So that, when ωt varies between $-\pi$ and π, $E_\perp(t)$ will oscillate twice between -140 and 140 kV/cm, passing through the anticrossing value periodically. Thus, there are two temporal intervals where only the first level is under the Fermi level (transitions $1\rightarrow2$ and $1\rightarrow3$ dominate) and three intervals where the two deepest subbands are occupied (the main transitions are $1\rightarrow3$ and $2\rightarrow3$). In the last case, temporal evolution of the subbands population and the corresponding depolarization shifts $[\alpha_{31}(t)$ and $\alpha_{32}(t)]$ have been considered in calculations. In this case, relaxation energy values are $\hbar\nu_{12}\simeq1.2$ meV, $\hbar\nu_{13}\simeq1.6$ meV, and $\hbar\nu_{23}\simeq1.9$ meV in the passive region, and $\hbar\nu_{12}\simeq4.5$ meV, $\hbar\nu_{13}\simeq4.5$ meV, and $\hbar\nu_{23}\simeq8.9$ meV in the active region. The absorption obtained is shown in Fig. 7 compared with the corresponding to $E_\omega=100$ kV/cm in order to easily ap-
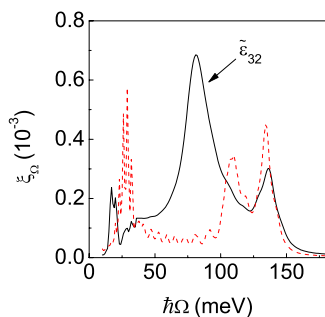
preciate the new peak related to $2\rightarrow3$ transition. Due to the high relaxation rates in the active region, it is not possible to appreciate any additional structure of the absorption. We have neglected the possible Γ-X mixing that could be induced by high electric fields.[19]

IV. SUMMARY

In summary, this work shows that the behavior of the relative absorption for multiple-GQWs, with very close excited levels, is essentially different to that of a simple multiple-QW when an intense terahertz irradiation is applied, showing a richer and complex structure due to the appearance of new transitions between the three involved levels. Results indicate how the zero-field peak is unfolded in two main peaks escorted by a series of satellites whose number increases with the field amplitude. Such a fine structure of the absorption is due to the $(n+1)$-order intersubband transitions, with n terahertz photons and a single IR photon. Also, a strong modification of absorption, which consists on a noticeable spreading of the fine structure, with a redshift of the left maximum and a blueshift of the right maximum for both transitions, is also demonstrated. The subbands depolarization shift has been considered. Effects caused when the two deepest subbands are populated are included leading to the appearance of a third peak.

Experimentally, the intense terahertz irradiation can be achieved by using free-electron or gas lasers with an energy density in the megawatt cm^{-2} range (applications of these lasers to study a heterostructure response can be found in Ref. 7 or Ref. 6, respectively). An alternative technique to experimentally investigate the above mentioned peculiarities of the relative absorption could be measures of the photoconductivity. Due to the importance of IR intersubband absorption in many electro-optical devices,[20] we expect the present results are useful in the designing of such devices and encourages researches to carry out experiments in this topic.

ACKNOWLEDGMENTS

APPENDIX A: DEPOLARIZATION SHIFT

When intersubband transitions are excited by the laser transverse electric field, electronic quantum states become a superposition of wave functions of the subbands involved in the transition. As a consequence, the charge density is inhomogeneously distributed along the z direction. This charge distribution is proportional to the electronic total density and induces a space-charge field that is superimposed to the laser driving field, changing the resonant frequency of the transition (interlevel distance). This frequency shift is called depolarization shift.

If we define the induced current density as

FIG. 7. (Color online) Relative absorption for $E_\omega=140$ kV/cm (solid line) and $E_\omega=100$ kV/cm (dashed line).

$$j_\perp(t,t') = \sum_j e\rho_{2D}v_{1j}(t)\int_0^\infty d\varepsilon\,\delta f_{1j}(\varepsilon,t')$$

$$= \sum_j ev_{1j}(t)[\mathcal{N}_{1j}(t') - \mathcal{N}_{j1}(t')], \quad \text{(A1)}$$

where the density-matrix elements satisfy the following equations

$$i\hbar\frac{\partial}{\partial t'}\mathcal{N}_{1j}(t') = -\varepsilon_{j1}(t)\mathcal{N}_{1j}(t') + \tilde{n}_{2D}\left\{i\frac{e}{\omega}v_{1j}(t)E_\perp(t') + \tilde{V}_{1j}(t)\right.$$

$$\left.\times[\mathcal{N}_{j1}(t') + \mathcal{N}_{1j}(t')]\right\},$$

$$i\hbar\frac{\partial}{\partial t'}\mathcal{N}_{j1}(t') = \varepsilon_{j1}(t)\mathcal{N}_{j1}(t') + \tilde{n}_{2D}\left\{i\frac{e}{\omega}v_{1j}(t)E_\perp(t') - \tilde{V}_{1j}(t)\right.$$

$$\left.\times[\mathcal{N}_{j1}(t') + \mathcal{N}_{1j}(t')]\right\}. \quad \text{(A2)}$$

where $\tilde{n}_{2D}(t) = \mathcal{N}_{11} - \mathcal{N}_{jj} = n_1(t) - n_2(t)$. Let us remember that we have chosen a parametrically time-dependent basis, $\varphi^k(z,t)$. Thus, interlevel velocity and energy depend on time through the wave functions. The term including the Coulomb matrix element $\tilde{V}_{1j}(t)$ details the renormalization of the external electric field caused by the charge redistribution within the heterostructure. Coulomb matrix element is connected to the wave functions of the two subbands through

$$\tilde{V}_{1j}(t) = \frac{4\pi e^2}{\epsilon}\int_{-\infty}^\infty dz\,\varphi^j(z,t)\varphi^1(z,t)\int_{-\infty}^z dz$$

$$\times\int_{-\infty}^{z'} dz''\,\varphi^j(z'',t)\varphi^1(z'',t). \quad \text{(A3)}$$

Adding and subtracting Eqs. (A2) and taking the second-order derivative of this difference, after some algebra, we obtain the Fourier component $(t' \to \omega)$ of the current as

$$j_\perp(\omega,t) = i\sum_j \frac{|ev_{1j}(t)|}{\omega}2\tilde{n}_{2D}(t)$$

$$\times\frac{2[\varepsilon_{j1}(t) + 2\tilde{n}_{2D}\tilde{V}_{1j}(t)]}{\varepsilon_{j1}^2(t) + 2\tilde{n}_{2D}\tilde{V}_{1j}(t)\varepsilon_{j1}(t) - (\hbar\omega)^2}E_\perp(\omega),$$

$$\quad \text{(A4)}$$

and finally,

$$j_\perp(\omega) = i\sum_j \int_{-\pi/\omega}^{\pi/\omega}\left\{\frac{|ev_{1j}(t)|}{2\pi}2\tilde{n}_{2D}(t)\right.$$

$$\left.\times\frac{2[\varepsilon_{j1}(t) + 2\tilde{n}_{2D}\tilde{V}_{1j}(t)]}{\varepsilon_{j1}^2(t) + 2\tilde{n}_{2D}\tilde{V}_{1j}(t)\varepsilon_{j1}(t) - (\hbar\omega)^2}\right\}$$

$$\times dtE_\perp(\omega) = \sigma(\omega)E_\perp(\omega). \quad \text{(A5)}$$

Expression (A5) indicates that the conductivity and, thus, the relative absorption has a singularity at $\varepsilon_{j1}^2(t) + 2\tilde{n}_{2D}\tilde{V}_{1j}(t)\varepsilon_{j1}(t) - (\hbar\omega)^2 = 0$ for each $1 \to j$ subband transi-

tion. This singularity can be prevented by including dissipative terms changing ω by $\omega - i\gamma$, where γ is the inverse of a characteristic relaxation time. Thus, the relative absorption has a maximum at $\hbar\omega = \sqrt{\varepsilon_{j1}^2(t) + 2\tilde{n}_{2D}(t)\tilde{V}_{1j}(t)\varepsilon_{j1}(t)}$ $= \varepsilon_{j1}(t)\sqrt{1 + 2\tilde{n}_{2D}(t)\tilde{V}_{1j}(t)/\varepsilon_{j1}(t)} = \varepsilon_{j1}(t)\sqrt{1 + \alpha_{j1}(t)}$. The depolarization shift is defined as $\Delta_{ds}(t) = [2\tilde{n}_{2D}(t)\tilde{V}_{1j}(t)\varepsilon_{j1}(t)]^{1/2}$ $= \varepsilon_{j1}(t)[\alpha_{j1}(t)]^{1/2}$, the amount that the peak maximum shifts from $\varepsilon_{j1}(t)$. By substituting $\tilde{n}_{2D}$ and $\tilde{V}_{1j}(t)$ we obtain, for our structure,

$$\Delta_{ds}(t) = \frac{8\pi e^2}{\epsilon}\varepsilon_{j1}(t)[n_1(t) - n_2(t)]\int_{-\infty}^\infty dz\,\varphi^j(z,t)\varphi^1(z,t)$$

$$\times\int_{-\infty}^z dz'\int_{-\infty}^{z'} dz''\,\varphi^j(z'',t)\varphi^1(z'',t). \quad \text{(A6)}$$

This expression is similar to Eq. (7).

APPENDIX B: INTERSUBBAND RELAXATION FREQUENCY

A detailed analysis of the interband relaxation frequency can be found in Refs. 14, 15, and 21. The dependence on time and density of this frequency can be obtained as follows.[22] If the intersubband collision integral in the kinetic equation of the matrix density if defined as $J(\delta f|\mathbf{p}) = -\nu\delta f_\mathbf{p}$, one obtains that the rate of electronic transitions from the state $|n\mathbf{p}\rangle$ to the subband n' is

$$\nu_{ij}(p,t) = \frac{2\pi}{\hbar}\sum_\mathbf{Q}|C_Q|^2|\langle j|e^{iq_z z}|i\rangle|^2$$

$$\times\{(N_Q + 1)\delta[\varepsilon_{ip}(t) - \varepsilon_{j\mathbf{p}-\hbar\mathbf{q}}(t) - \hbar\omega_Q]$$

$$\times(1 - f_{j\mathbf{p}-\hbar\mathbf{q}}) + N_Q\delta(\varepsilon_{ip} - \varepsilon_{j\mathbf{p}-\hbar\mathbf{q}} - \hbar\omega_Q)$$

$$\times(1 - f_{j\mathbf{p}+\hbar\mathbf{q}})\}, \quad \text{(B1)}$$

where $\mathbf{Q} = (\mathbf{q}, q_z)$ is phonon wave number, N_Q is the phonon distribution function, L is the normalization area, and $\mathbf{p}$ is the electronic momentum. For the elastic-scattering case $(\hbar\Omega < \hbar\Omega_{LO})$ we substitute the coupling factor for the deformation-potential interaction with the acoustic phonons, C_Q. Neglecting Pauli blocking $(1 - f_{j\mathbf{p}\mp\hbar\mathbf{q}})$, and integrating over q_z we get

$$\nu_{ij'}^{LA}(p,t) = \frac{2\pi D^2 T}{\hbar\rho s^2 L^2}\int_{-\infty}^\infty dz[\varphi^i(z,t)]^2[\varphi^j(z,t)]^2\sum_\mathbf{q}$$

$$\times\delta\left[\varepsilon_{ij}(t) + \frac{\hbar\mathbf{p}\cdot q}{m} - \frac{\hbar^2 q^2}{2m}\right]. \quad \text{(B2)}$$

where D is the deformation potential, ρ is the crystal density, and s the sound velocity in the sample. To integrate we have used the parabolic energy dispersion $\varepsilon_{ip}(t) = \varepsilon_i(t) + p^2/2m$ and $\varepsilon_{ij}(t) = \varepsilon_i(t) - \varepsilon_j(t)$. Now we define $\mathbf{p}' = p - \hbar\mathbf{q}$ and the sum over $\mathbf{q}$ can be written as $\sum_q\delta[\varepsilon_{ij}(t) + \varepsilon_p - \varepsilon_{p'}]$. By using 2D density of states we obtain

$$\nu_{ij}^{LA}(t) = \frac{\pi D^2 T \rho_{2D}}{\hbar s^2 \rho} \int_{-\infty}^{\infty} dz [\varphi^i(z,t)]^2 [\varphi^j(z,t)]^2. \quad \text{(B3)}$$

Here, $\int_{-\infty}^{\infty} \frac{dq}{2\pi} |\langle i|e^{-iqz}|j\rangle|^2 = \int_{-\infty}^{\infty} dz [\varphi^i(z,t)]^2 [\varphi^j(z,t)]^2$ are the characteristic intersubband wave vectors with self-consistent wave functions. Thus, $\nu_{ij}(t)$ depends on the electronic density through self-consistent wave functions, which include electron-electron interaction. When the sample is subjected to a terahertz irradiation with frequency ω, we average along a period and finally obtain

$$\nu_{ij}^{LA}(\omega) = \int_{-\pi/\omega}^{\pi/\omega} \frac{dt}{2\pi/\omega} \nu_{ij}^{LA}(t). \quad \text{(B4)}$$

Thus, the relaxation frequency depends on the electronic density and the frequency of the terahertz field.

In the active region ($\hbar\Omega > \hbar\Omega_{LO}$), the relaxation frequencies can be obtained by substituting $C_Q = \sqrt{2\pi e^2 \hbar \omega_{LO}/\epsilon q^2 V}$ from the Frölich interaction with long-wavelength longitudinal optical phonons. Neglecting Pauli blocking and for the low-temperature case (we neglect absorption and stimulated emission of LO phonons),

$$\nu_{ij}^{LO}(p,t) = \frac{2\pi^2 e^2 \hbar \Omega_{LO}}{\epsilon^* L^2} \sum_{\mathbf{q}} \int_{-\infty}^{\infty} dz$$
$$\times \frac{e^{-q|z-z'|}}{q} \varphi^i(z,t) \varphi^j(z,t) \varphi^i(z',t) \varphi^j(z',t)$$
$$\times \delta \left[\varepsilon_{nn'}(t) - \hbar\omega_{LO} + \frac{\hbar \mathbf{p} \cdot \mathbf{q}}{m} - \frac{\hbar^2 q^2}{2m} \right], \quad \text{(B5)}$$

where $\epsilon^* = \frac{1}{\epsilon_\infty} - \frac{1}{\epsilon_0}$ is effective dielectric constant. Integrating over the angle of $\mathbf{q}$,

$$\nu_{ij}^{LO}(p,t) = 2\Omega_{LO} \frac{\epsilon}{\epsilon^*} \int_{q_{min}}^{q_{max}} dq \frac{q M_{ijij}(q,t)}{[(q^2 - q_{min}^2)(q_{max}^2 - q^2)]^{1/2}}, \quad \text{(B6)}$$

with $\hbar q_{min}(t) = |p - \sqrt{p^2 + \tilde{p}_{ij}^2(t)}|$, $\hbar q_{max}(t) = p + \sqrt{p^2 + \tilde{p}_{ij}^2(t)}$, $\tilde{p}_{ij}^2(t) = p_{ij}^2(t) - p_{LO}^2$, $p_{LO} = \sqrt{2m\hbar\Omega_{LO}}$, and $p_{ij}^2(t) = 2m\varepsilon_{ij}(t)$. The matrix $M_{ijij}(q,t)$ is defined as

$$M_{ijkl}(q,t) = \frac{e^2 m}{\pi \epsilon \hbar^2} \int_{-\infty}^{\infty} dq_z \frac{\langle i|e^{-iq_z z}|j\rangle \langle k|e^{iq_z z}|l\rangle}{q^2 + q_z^2}$$
$$= \frac{e^2 m}{\pi \epsilon \hbar^2 q} \int_{-\infty}^{\infty} dz \varphi^i(z,t) \varphi^j(z,t)$$
$$\times \int_{-\infty}^{z} dz' \varphi^k(z',t) \varphi^l(z',t) e^{-q|z-z'|}. \quad \text{(B7)}$$

Some approximations can be done if $p \ll p_{ij'}$, as in photoexcitation. In this case, q is fixed due to the energy conservation law and $M_{ijij}(q,t)$ only depends on time and electronic density. Now Eq. (B6) reduces to

$$\nu_{ij}^{LO}(t) = \pi\Omega_{LO} \frac{\epsilon}{\epsilon^*} \frac{\sqrt{|2m[\varepsilon_{ij}(t) - \hbar\Omega_{LO}]|}}{\hbar}$$
$$\times \int_{-\infty}^{\infty} dz \varphi^i(z,t) \varphi^j(z,t)$$
$$\times \int_{-\infty}^{z} dz' \varphi^i(z',t) \varphi^j(z',t) |z - z'|. \quad \text{(B8)}$$

and averaging over a period,

$$\nu_{ij}^{LO}(\omega) = \int_{-\pi/\omega}^{\pi/\omega} \frac{dt}{2\pi/\omega} \nu_{ij}^{LO}(t). \quad \text{(B9)}$$

Again relaxation rate depends on terahertz frequency and electronic density.

---

*ajhernan@ull.es

[1] S. D. Ganichev and W. Prettl, *Intense Terahertz Excitation of Semiconductors* (Clarendon, Oxford, 2005).

[2] H. Haug and S. W. Koch, *Quantum Theory of the Optical and Electronic Properties of Semiconductors* (World Scientific, Singapore, 1994); F. T. Vasko and A. V. Kuznetsov, *Electron States and Optical Transitions in Semiconductor Heterostructures* (Springer, New York, 1998).

[3] A.-P. Jauho and K. Johnsen, Phys. Rev. Lett. **76**, 4576 (1996); K. Johnsen and A.-P. Jauho, Phys. Rev. B **57**, 8860 (1998); Phys. Rev. Lett. **83**, 1207 (1999).

[4] M. Helm, in *The Basic Physics of Intersubband Transitions*, Semiconductors and Semimetals Vol. 62 (Academic, London, 2000), p. 1.

[5] A. Hernández-Cabrera, P. Aceituno, and F. T. Vasko, Phys. Rev. B **72**, 045307 (2005).

[6] Z. Y. Lai and W. Z. Shen, J. Appl. Phys. **94**, 367 (2003); S. D. Ganichev and W. Prettl, J. Phys.: Condens. Matter **15**, R935 (2003).

[7] M. Y. Su, S. G. Carter, M. S. Sherwin, A. Huntington, and L. A. Coldren, Phys. Rev. B **67**, 125307 (2003).

[8] H. X. Li, Z. G. Wang, J. B. Liang, B. Xu, J. Wu, Q. Gong, C. Jiang, F. Q. Liu, and W. Zhou, J. Appl. Phys. **82**, 6107 (1997); C. C. Yang, K. C. Huang, and Y. K. Su, Jpn. J. Appl. Phys., Part 2 **35**, L535 (1996).

[9] A. C. H. Lim, R. Gupta, S. K. Haywood, M. J. Steer, M. Hopkinson, and G. Hill, Appl. Phys. Lett. **89**, 261110 (2006).

[10] A. Hernández-Cabrera, P. Aceituno, and F. T. Vasko, Phys. Rev. B **67**, 045304 (2003).

[11] V. L. Zerova, G. G. Zegrya, and L. E. Vorob'ev, Semiconductors **38**, 1053 (2004); V. L. Zerova, G. G. Zegrya, and L. E. Vorob'ev, *ibid.* **38**, 689 (2004).

[12] S. J. Allen, D. C. Tsui, and B. Vinter, Solid State Commun. **20**, 425 (1976).

[13] P. Aceituno and A. Hernández-Cabrera, J. Appl. Phys. **98**, 013714 (2005).

[14] I. Waldmüller, J. Förstner, S.-C. Lee, A. Knorr, M. Woerner, K. Reimann, R. A. Kaindl, T. Elsaesser, R. Hey, and K. H. Ploog, Phys. Rev. B **69**, 205307 (2004).

[15] M. F. Pereira, Jr., S.-C. Lee, and A. Wacker, Phys. Rev. B **69**, 205310 (2004); M. F. Pereira, Jr. and H. Wenzel, *ibid.* **70**, 205331 (2004).

[16] M. Załużny, Phys. Rev. B **47**, 3995 (1993).

[17] H. Yldirim and M. Tomak, Phys. Status Solidi B **243**, 2874 (2006).

[18] A. A. Batista, P. I. Tamborenea, B. Birnir, M. S. Sherwin, and D.

S. Citrin, Phys. Rev. B **66**, 195325 (2002).

[19] J. P. Hagon, M. Jaros, and D. C. Herbert, Phys. Rev. B **40**, 6420 (1989).

[20] O. Wada, New J. Phys. **6**, 183 (2004); A. J. F. Levi, Proc. IEEE **96**, 335 (2008); I. Hosako, N. Sekine, M. Patrashin, S. Saito, K. Fukunaga, Y. Kasai, P. Baron, T. Seta, J. Mendrok, S. Ochiai, and H. Yasuda, *ibid.* **95**, 1611 (2007).

[21] M. F. Pereira, Jr., Braz. J. Phys. **32**, 940 (2002).

[22] F. T. Vasko and O. E. Raichev, *Quantum Kinetic Theory and Applications: Electrons, Photons and Phonons* (Springer, New York, 2004).